Interstellar Astrophysics
Summary notes: Part 4

Dr. Paul M. Woods

The main reference source for this section of the course is Chapter 3 in the Dyson and Williams (The Physics of the Interstellar Medium) book. Beware: this book is very technical!!

Note: Figure numbers refer either to the chapter and figure number (N-n) in Freedman and Kauffman, or to the Dyson and Williams textbook.

3 Diffuse interstellar clouds

3.1 Heating and cooling mechanisms

The hydrogen that is found deep inside diffuse clouds is almost entirely neutral (apart from a small proportion that is ionised by X-rays from the hot interstellar medium (HIM) penetrating into the clouds).

Even if an OB star (or stars) were nearby, **no** UV photons at wavelengths less than 912 Å can penetrate deep into these diffuse clouds, since (be definition) they will have ALL been used up in ionising the outer H. Thus deep in these diffuse clouds we cannot invoke H-photoionisation as the main heating mechanism. Only atoms with Ionization Potentials (IPs) less than 13.6 eV can be ionised by the remaining lower energy photons. Helium (the next most abundant element) has IPs even higher than for H (24 eV for neutral He and 54 eV for He^+), so photoionisation of this element is impossible. O I and N I have IPs of 13.6 eV and 14.4 eV, so again these elements are unsuitable. Neutral C, (C I) does have a lower IP (11.3 eV, corresponding to a wavelength of 1110 Å) so potentially photoionisation of C I could provide KE of photoelectrons which could heat the gas.

However, photoionisation of C I is NOT an efficient heating process since: (a) C I is not very abundant ($\sim 10^{-4}$ that of H), (b) only a small range of photons between 912–1110 Å are available to photoionise the C I, and (c) the maximum KE we can obtain from this process would be $13.6 - 11.3$ eV $= 2.3$ eV, which is quite low.

The main heating process for the deep layers within the diffuse ISM is the ejection of 'photoelectrons' from the small dust grains that exist with the gas*. Such grains have a

*called 'photoelectrons' because they are produced by the impact of photons on the dust grain surface – the Photoelectric Effect relatively low **work function** (analogous to atomic Ionisation Potential energy), denoted W. The energy, E, of the ejected electron is thus:

$$E = h\nu - W$$

– h is the Planck constant (6.62×10^{-34} J s)
– ν is the photon *frequency*

Small grains have $W \sim 5$ eV, which will give typical values of kinetic energy of the photoejected electrons of ~6 eV. This KE is shared with other particles by collisions, which thermalises the gas and heats it.

Cooling of the diffuse ISM gas is again mainly due to Forbidden Line emission, particularly in low-lying states in neutral O I and, especially in singly ionised carbon, C II. Very strong forbidden lines occur in the far-infrared: C II 158 μm, O I 146 μm.

Putting in the dust grain heating rates and forbidden line cooling rates for typical diffuse ISM cloud densities of $n \sim 10^8$ m^{-3} gives estimates of kinetic temperatures of ~70–100 K.

3.2 Absorption line spectroscopy of interstellar medium gas

Not all ISM material emits brightly. If it is cold or of low density, then line emission will be weak. However, we still want to understand what the properties of this gas are. How can we do this if we can't see it? The answer is to use a bright background source (e.g. a star, AGN, or quasar) in order to see foreground ISM in 'silhouette'. Silhouetted dark clouds can easily be seen in photographs of nebulae. Here, however, we use the word 'silhouette' to mean a spectral absorption line.

When we observe the spectrum of a bright background source we are seeing: (i) the intrinsic spectrum emitted from the e.g. stellar atmosphere and (ii) superimposed on this the effects of the intervening interstellar medium lying between the it and us (see Fig. 20-5). The ISM material will consist of both gas and dust particles. The dust tends to scatter and absorb the UV/optical radiation from the star causing a reddening and extinction of the starlight.

The atoms and ions of the different elements that make up the gas in the intervening ISM material can absorb the background source's radiation at specific wavelengths corresponding to different electronic transitions in the gas atoms giving interstellar absorption lines superimposed on the intrinsic stellar spectrum. A study of these ISM absorption lines can reveal many of the physical and chemical properties of the line-of-sight ISM gas: its temperature, line-of-sight motion(s) (velocity), density, and (especially) the chemical composition of the ISM gas.

The low density of ISM gas means that the gas atoms and ions are in a very low excitation state, such that all the electrons can be assumed to be in the atom/ion ground state. Thus absorption of background star photons can only involve a transition FROM the ground state to some excited bound level. Such $n = 1 \rightarrow n'$ transitions are called **resonance**

transitions and the corresponding spectral lines are denoted as **resonance lines**. In hydrogen, the resonance lines are the Lyman lines: e.g. Lyα 1215 Å, Lyβ 1025 Å, Lyγ 972 Å, etc.

It turns out from the basic physics of the atomic structure of atoms, that with the exceptions of ionised calcium and neutral sodium†, all atoms/ions of most of the chemical elements have their resonance lines occurring at ultraviolet wavelengths, in the UV (1200–3300 Å), the Far-UV (912–1200 Å) and in the Extreme-UV (100–912 Å). Such UV/FUV/EUV radiation is absorbed by the Earth's atmosphere and thus requires observations from space to see these resonance lines. The most useful satellites for such data have been the International Ultraviolet Explorer (IUE) and the Hubble Space telescope (HST) for UV spectroscopy, and the Far-Ultraviolet Spectroscopic Explorer (FUSE) satellite for FUV data.

Hot OB stars are often used as probes of the ISM gas within our Galaxy, since: (i) they have a relatively simple intrinsic spectrum with little neutral atom or low ionization stage photospheric absorption spectra, (ii) copious emergent flux at UV/FUV/EUV wavelengths which can be absorbed by the ISM gas resonance lines which occur at these wavelengths (see above), and (iii) the stars are very luminous, up to a million times that of the Sun, and thus can be seen to large distances in the Galaxy, and thus can be used as background probes of the ISM to large distances.

3.2.1 Gas phase elemental abundances in cold ISM clouds from UV spectroscopy

The absorption strength of an individual spectral line depends upon, to a first approximation, its atomic transition probability multiplied by the number of absorptions along the line of sight. The latter is determined by the column density (N) of absorbing atoms along the line of sight, which is roughly given by the number density of atoms multiplied by the distance along the line of sight (ℓ), i.e.

$$N(\text{absorber}) = n(\text{absorber}) \ \times \ \ell$$

The overall strength of absorption of a single line is often measured in terms of its equivalent width, W_λ. W is defined to be the width of a strip of continuum, of intensity I_c, which has the same area as under the absorption line profile – see Fig. 1.

For relatively weak absorption lines the equivalent width is proportional to N. As we increase N, so W will increase linearly. In fact, once a line becomes very strong the absorption near the line centre reaches zero intensity (saturation), and for some further increase in N, W only increases marginally. Thereafter an increase in column density produces a somewhat slower increase in W compared to the linear effect for weak lines. The overall behaviour of W with increasing N is called a curve of growth, and can be theoretically computed (Fig. 2).

† Ca II 3968, 3933 Å, Na I 5895 Å resonance lines are in the optical part of the spectrum. These are Fraunhofer lines.

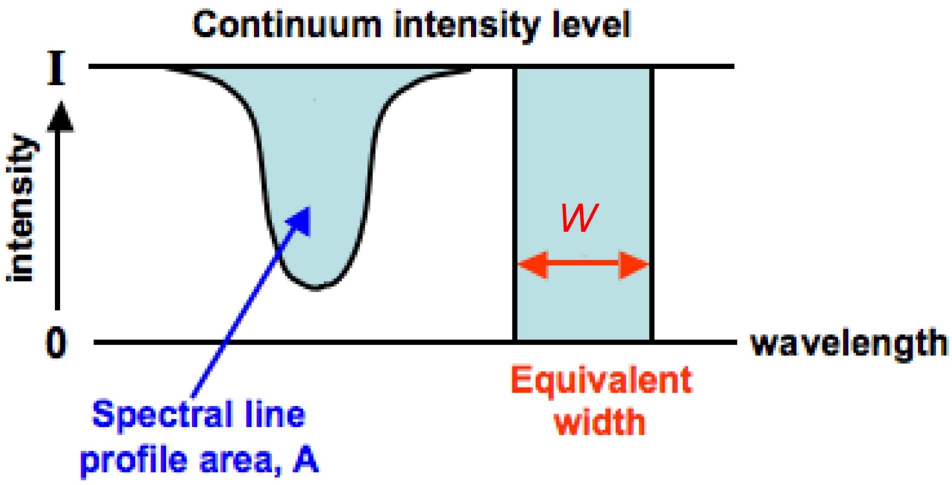

Figure 1: Definition of 'equivalent width'.

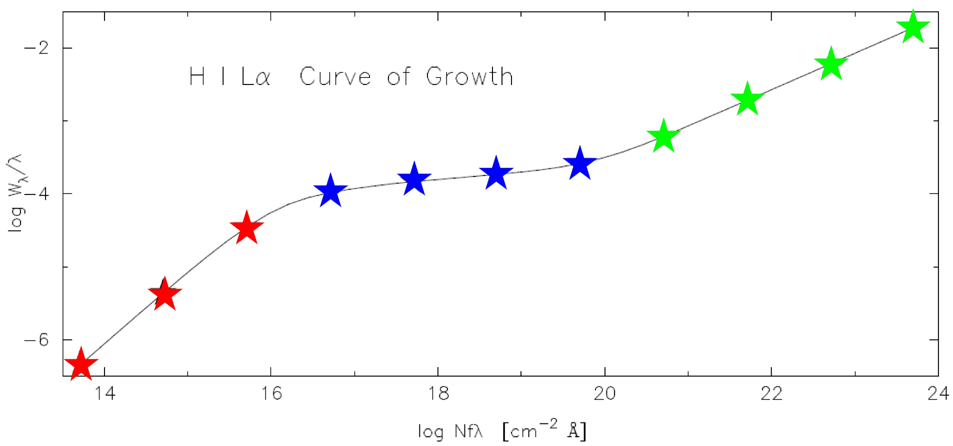

Figure 2: H I Lyα curve of growth. Red stars indicate the linear ($\propto$ N) part, blue stars indicate the flat part, and green stars indicate the damping ($\propto \sqrt{\mathrm{N}}$) part.

The basic approach to the determination of gas phase element abundances is as follows:

(i) obtain a high spectral resolution spectrum (with resolving power‡ $R > 10\,000$ in the UV/FUV using a satellite like IUE/HST/FUSE) of a suitable background OB star.

(ii) identify in the observed spectrum a set of ISM resonance absorption lines using laboratory line lists of resonance lines of different elements, using the observed and lab wavelengths – small shifts in wavelength between that observed and the lab indicate absorption in a ISM cloud moving at some relative velocity between the star and the earth, and thus gives knowledge of the dynamics of the individual ISM clouds,

(iii) from the observed spectrum measure the equivalent widths of a set of lines from different elements, and use a curve of growth to get the column density for each element, $N_{\rm elem}$,

(iv) from determinations of the hydrogen column density in the cloud (e.g. from the Lyman resonance line absorptions) derive abundances relative to hydrogen for each element in the gas. These are called **fractional abundances**.

3.2.2 Gas phase element depletion

It is found that most elements in the gas phase are under-abundant relative to hydrogen compared to normal Solar abundances, often by factors of 100 to 1000. This is especially the case for elements like O, Fe, Mg, Si, Al, (but often less so for elements like S, N).

This result is generally true for all sight lines throughout the Galaxy (and in other galaxies like the Magellanic Clouds) and is the result of a depletion of these elements from the gas phase onto dust grains which are mixed up with the gas. Thus elemental depletions deduced from UV ISM spectra thus tells us something about the chemical composition of the dust itself.

In very high resolution spectra, we can often see for an individual spectral line transition, multiple absorptions separated by small amounts in wavelength, or blended to form a broadened line profile. This reflects absorption in the same line transition occurring in more than one line-of-sight cloud, with the different clouds having different velocity relative to the Earth. If the data is of sufficient quality, in terms of spectral resolution and signal-to-noise, such multi-absorption line data can be modelled to determine the abundances and relative motions of the different clouds in the gas in the line of sight.

4 Interstellar dust and extinction

We saw that the gas phase of the ISM shows element abundances with strong depletions of compared to normal solar abundances, particularly in C, Si, Al, Fe etc., due to these elements being locked up in dust grains.

‡Resolving power, R, is defined as $R = \lambda/\Delta\lambda$, where $\Delta\lambda$ is the instrumental width of the line.

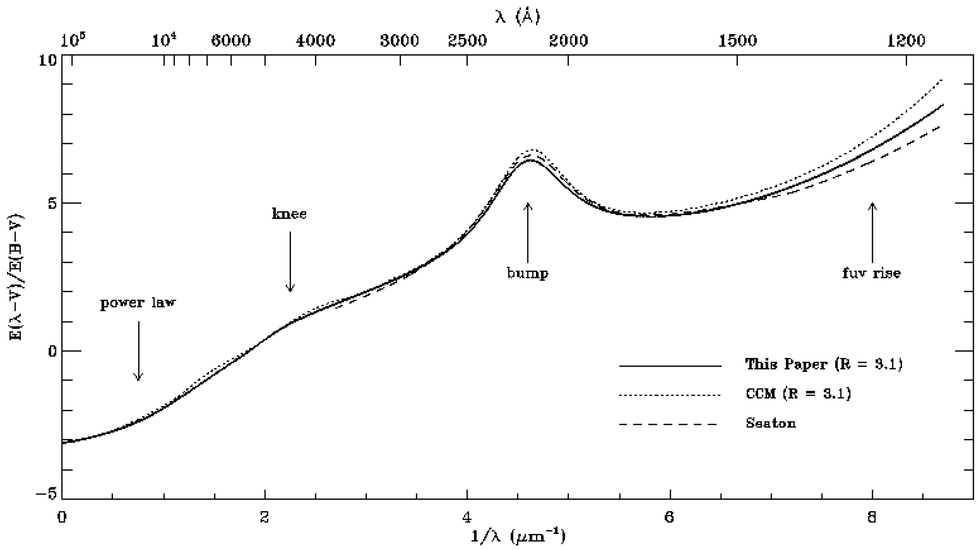

Figure 3: Average interstellar extinction curve (solid line). Note: always plotted against *inverse* wavelength for historical reasons!

Other evidence for the existence of dust in the general ISM comes from direct imaging at optical wavelengths of dark patches on the sky (see Figs. 20-2 and 20-3). These dark patches, like the Horsehead Nebula in Orion, have relatively dense concentrations of dust particles that scatter and absorb light very efficiently. Typical dark nebula have densities of $n \sim 10^4$–10^9 cm^{-3}and low temperatures, $T \sim 10$–$100\,$K, which are dense enough to block the passage of background light.

Other imaging evidence for dust comes from reflection nebulae (e.g. Fig. 20-2) which appear bluish due to the scattering of starlight from nearby (not embedded) OB stars, where the blue starlight is scattered more than red light by the small dust grains.

The dust in the ISM also alters the observed energy distributions of background stars causing interstellar reddening. Examples are shown in the differences between the UV-optical flux distributions observed between stars of the same spectral types but at different distances. The more distant stars show more “reddened” energy distributions due to the scattering and absorption by dust in the ISM line of sight (N.B.: intrinsically the stars of the same spectral type would have the same flux distributions). By comparing the flux distributions of reddened and unreddened stars of the same spectral types one can directly determine the wavelength dependence of the dust scattering/absorption properties – the interstellar extinction law.

This curve is shown in Fig. 3 (see also Fig 4.2 of Dyson and Williams). The attenuation of light at a particular wavelength, λ, is A_λ. Subtracting the flux at one wavelength from another gives a **colour**. We therefore define the colour excess as $E(B-V) = (B-V) - E(B-V)_0$, where $E(B-V)_0$ is the intrinsic colour of the object (e.g. star). In the V-band (∼500 nm), $A_{\lambda=V} \sim 3.2\,E(B-V)$.

The dust extinction increases from nearly zero at IR wavelengths, through to values of $\mathrm{A}_V/\mathrm{E}(B-V) \approx 3$ at the V-band to very large values of ∼10 in the far-UV near 1000 Å. The extinction curve also has a very strong absorption band centered at about 2200 Å,

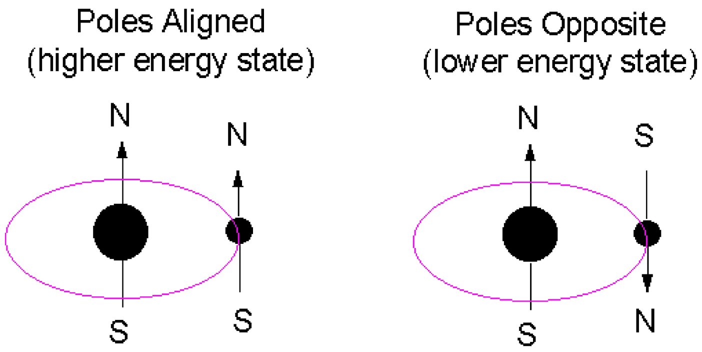

Figure 4: Spin (magnetic orientation) for neutral atomic hydrogen. The 'spins' of the proton and electron can either be parallel or antiparallel. A 'flip' between the higher energy parallel and lower-energy antiparallel state emits a photon with wavelength 21 cm (or frequency 1420 MHz).

which is very broad (about 400 Å), and is still unidentified (but may be due to graphite grains absorption).

In the IR, the dust extinction is very low, but there are several, quite strong, absorption features which spectra from the ISO satellite found to be due to grains like silicates (strong absorption near 10 μm) like magnesium-silicate, Mg_2SiO_4 or iron-silicate $FeSiO_4$. At about 3 microns, absorption features due to ice are also seen as well as solid state CO.

With knowledge of the extinction law, we can reverse the procedure, and use the level of extinction to derive a distance.

4.1 Interstellar radio emission

4.1.1 Neutral hydrogen emission

Neutral hydrogen consists of a single proton orbited by a single electron. As well as their orbital motion, the proton and electron also have a quantum mechanical property called spin. The spin of the electron and proton can be in either direction – in the classical analogy they are rotating clockwise or anticlockwise around a given axis. When the spins of the electron and proton aligned in the same direction (parallel), the hydrogen atom has slightly more energy than when the spins in opposite directions (anti-parallel). This is because of complex magnetic interactions between the particles.

When an electron changes its 'spin' from parallel to anti-parallel, this results in the atom losing energy – this energy is emitted in the form of a photon with a wavelength 21 cm (or 1420 MHz) – see Fig. 4. This transition is highly forbidden with an extremely small probability of occurring (2.9×10^{-15} s^{-1}). This means that the average time a single isolated atom of neutral hydrogen would take to undergo this transition would be around 10 million years, and so is unlikely to be seen in a laboratory on Earth. However, as the total number of atoms of neutral hydrogen in the interstellar medium is very large, this emission line is easily observed.

4.2 Giant molecular clouds

Where do stars form in the Galaxy? Nearby dark nebulae (e.g. in Orion) can be silhouetted against background stars or H II regions, but more distant dark nebulae cannot be seen in this way because of interstellar extinction. At long wavelengths such ISM extinction becomes very low, and the ISM dust becomes transparent at far-IR and radio wavelengths (mm, cm wavelengths).

In cold clouds the temperatures are low enough for molecules to form, and just like atoms, molecules can emit spectral lines. The spectral features of molecules in interstellar space are generated by electron transitions between different energy levels, or by rotational or vibrational energy changes. Their emission lines generally lie in the radio, microwave, or infrared portions of the spectrum. The first molecule to be detected in the interstellar medium was the methylidyne radical (CH) in 1937 by by Swings & Rosenfeld.

Using radio telescopes and mm-wave telescopes (like the JCMT on Hawaii), more than 100 molecular species have now been detected in the ISM gas. Table 1 lists some of the most common molecules found in the ISM.

The most abundant molecule is molecular hydrogen (H_2), but this has no radio frequency lines (it does have some near 2 μm, and its resonance lines are in the far-UV). Carbon monoxide (CO) is the next most abundant molecule, and has lines at 2.6 mm. We can take advantage of the fact that the ratio of CO to H_2 is fairly constant throughout the (local) Universe ($CO/H_2 \sim 10^{-4}$), and use much more observable transitions from CO to trace the cold, dense molecular hydrogen gas. Surveys of CO emission in the Galaxy show that the CO is largely concentrated in Giant Molecular Clouds (GMCs). These have diameters of typically 15–100 pc, masses $\sim 10^5$–10^6 $M_\odot$, and densities of ~ 200 H_2 molecules cm^{-3}. The Galaxy contains at least 5 000 GMCs.

Fig. 20-19 shows the CO maps of the Orion region – note the large areas covered by the molecular clouds. Fig 20-20 shows a schematic location of the GMCs in the Galaxy – which are found to trace the spiral arms – very similar to the location of H II regions around OB stars (which have been recently formed). It is this very evident that spiral arms are the sites of new star formation.

Table 1: Selected interstellar molecules

Complexity	Inorganic		Organic	
Diatomic	H_2	hydrogen	CH	methylidyne radical
	OH	hydroxyl radical	CN	cyanogen radical
	SiO	silicone monoxide	CO	carbon monoxide
	SO	sulphur monixide	C_2	carbon
	NO	nitric oxide	CS	carbon monosulphide
Triatomic	H_2O	water	CCH	ethynyl radical
	H_2S	sulphur dioxide	HCN	hydrogen cyanide
	SO_2	sulphur dioxide	HCO	formyl radical
4-atomic	NH_3	ammonia	H_2CO	formaldehyde
			HNCO	hydrocyanic acid
			H_2CS	thioformaldehyde
5-atomic			CH_4	methane
			HCOOH	formic acid
$\vdots$			$\vdots$	$\vdots$
13-atomic			$HC_{11}N$	cyanopentaacetylene